

High Resolution Computed Tomography Finding in 552 Patients with Symptomatic COVID-19: First Report from North of Iran

CURRENT STATUS: POSTED



Hadi Majidi

Department of Radiology, Faculty of Medicine, Mazandaran University of Medical Sciences, Sari, Iran.

Elham-Sadat Bani-Mostafavi

Department of Radiology, Faculty of Medicine, Mazandaran University of Medical Sciences, Sari, Iran.

Zahra Mardanshahi

Department of Radiology, Faculty of Medicine, Mazandaran University of Medical Sciences, Sari, Iran.

Farnaz Godazandeh

Department of Radiology, Faculty of Medicine, Mazandaran University of Medical Sciences, Sari, Iran.

Roya Gasemian

Department of Radiology, Faculty of Medicine, Mazandaran University of Medical Sciences, Sari, Iran.

Keyvan Heydari

Student Research Committee, Mazandaran University of Medical Sciences, Sari, Iran

Reza Alizadeh-Navaei

Gastrointestinal Cancer Research Center, Mazandaran University of Medical Sciences, Sari, Iran

✉ reza_nava@yahoo.com *Corresponding Author*
ORCID: <https://orcid.org/0000-0003-0580-000X>

DOI:

10.21203/rs.3.rs-25817/v1

SUBJECT AREAS

Nuclear Medicine & Medical Imaging

KEYWORDS

Corona virus 2019, Ground glass, Peripheral distribution, Pleural effusion

Abstract

Purpose: Due to the emergence of the new Coronavirus-2019 and the lack of sufficient information about infected patients, this study was conducted to investigate the Chest High Resolution Computed Tomography (HRCT) findings of patients infected with the new *Coronavirus* 2019.

Methods: This cross-sectional study was performed on COVID-19 patients referred to Medical Imaging Centers of Sari, Mazandaran, Iran, on March 2020 for Computed Tomography Scan (CT-Scan). Symptomatic patients were referred to the Medical Imaging Center for diagnosis confirmation through CT-scan. In addition to age and sex, HRCT findings were collected from the picture archiving and communication system (PACS) for further evaluations.

Results: Out of 552 patients with mean age of 14.8 ± 51.2 years, the male/female ratio was 1.38 to 1. The most common expressive findings in patients were ground-glass opacity (GGO) (87.3%), peripheral distribution (82.4%) and posterior distribution (81.5%). The most conflicting findings in patients were pleural effusion (7.6%), peribronchovascular distribution (7.6%), and lymphadenopathy (5.1%). The peripheral distribution ($p = 0.034$), round opacities ($p = 0.02$), single lobe ($p = 0.003$) and pleural effusion ($p = 0.037$) were significantly in people under and over 50 years of age.

Conclusion: In summary, the present study indicated that in addition to GGO, peripheral distribution findings could be a vital diagnostic choice in COVID-19 patients.

Introduction

The COVID-19 is a novel heat-sensitive coronavirus. Based on evolutionary research, it has been found that the virus has originated from animals like bats, rodents and birds [1]. In early December 2019, the first cases of pneumonia of unknown etiology were observed in Wuhan, the capital of Hubei Province in China [2]. The pathogen, which was a single-stranded enveloped coronavirus RNA [3], was called acute respiratory syndrome coronavirus 2 (SARS-CoV-2), and the course of the disease caused by the virus is pathologically somewhat similar to that of severe acute respiratory syndrome (SARS) [4]. So far, seven types of coronaviruses have been identified that can infect humans [4-6]. Viruses that cause severe acute respiratory syndrome (SARS), Middle East respiratory syndrome (MERS), and the coronavirus disease (COVID-19) have zoonotic origins [6] and are transmitted from person to

person [7]. About 13.9% of patients with COVID-19 died and about half of those who visited hospitals were discharged after receiving the necessary treatment [8]. According to the study by Guan et al., 1099 patients in 552 hospitals with COVID-19 and an average age of 47 years were examined. Common manifestations of the virus include fever above 37.5 °C (56.2%), cough (67.8%), and lymphocytopenia (83.2%) [9]. According to several studies that examined the imaging findings of COVID-19 patients, 69 to 89% of the patients had positive chest CT findings [10, 11]. Ground-glass opacity (GGO) is frequently observed which has been reported in most studies [12, 13]. Radiological evaluation often plays a key role in confirming the diagnosis of COVID-19 in suspected cases when test kits are not available. Given the recency of the virus and the lack of sufficient information on patients involved in COVID-19 in Iran, during this study, the imaging findings of patients with COVID-19 were examined in Mazandaran province, located in the north of Iran.

Materials And Methods

This cross-sectional study was conducted in March 2020 on symptomatic patients who visited the imaging centers of Sari during the coronavirus epidemic. The study population were patients with high clinical suspicion who performed a CT scan because of limited laboratory testing in Iran to confirm the diagnosis and treatment. The CT scanner was a Somatom Emotion 16 by Siemens with a 16-slice configuration. The high-resolution computed tomography (HRCT) in axial sections was used without the contrast material with section thickness of 3 mm. The low-dose protocol (low-dose computed tomography) with radiation conditions of Kvp=100-120, mAs=50-100 and pitch=1mm was used. The patient was supine in the CT scanner with his/her arm above their head. CT scanning started from the apex to the lowest part of the lungs in a deep inspiration.

The required information, including demographic data such as age, gender, and HRCT results, was collected and recorded in a researcher-made checklist by four radiologists using the PACS system. Data were analyzed in SPSS 20 using t-test, chi-square and Fisher's exact tests and a $p < 0.05$ was considered as significant. Finally, due to the very different sample size in the literature, meta-analysis was undertaken using random effect method and Stata software to better compare the reported percentages.

Results

The study was conducted on 552 symptomatic patients with clinical suspicion who visited for HRCT.

The mean age of participants was 51.2 ± 14.8 years, in the range of 16 to 99 years, and the age group of 50 to 59 years with the relative frequency of 25.4% showed the highest involvement (Figure 1). In this study, 317 males (57.4%) and 235 females (42.6%) participated with a male/female sex ratio of 1.38.

The most common suggestive findings in patients were ground glass opacity (482 cases, 87.3%), peripheral distribution (455 cases, 82.4%), posterior distribution (450 cases, 81.5%) and anterior distribution (325 cases, 58.9%) (Table 1 and Figure 2). There was no significant difference between patients of both genders in the distribution of suggestive findings. Peripheral distribution (86% vs 79%, $p=0.034$) along with the findings of round opacity (19.5% vs 12.5%, $p=0.02$) and single lobe (23.2% vs 13.2%, $p=0.003$) was significantly higher in patients under 50 compared to those over 50 (Table 1).

The most common inconsistent findings in the study population were pleural effusion (42 cases, 7.6%), peribronchovascular distribution (42 cases, 7.6%), and lymphadenopathy (28 cases, 5.1%) (Table 2 and Figure 2). There was no significant difference between patients of both genders in the distribution of inconsistent findings. The age distribution of inconsistent findings indicated that pleural effusion was significantly higher ($p = 0.037$) in patients over 50 years of age (28 cases, 10%) compared to those under 50 (14 cases, 5.2%) (Table 2).

Figure 1. Age distribution of patients with coronavirus 2019

Table 1. Suggestive findings in HR CT-scan of symptomatic patients infected with coronavirus 2019

Findings	Total n=552 Frequency (%)	Female n=235 Frequency (%)	Male n=317 Frequency (%)	p-value	Age ≤50 n=271 Frequency (%)	Age >50 n=281 Frequency (%)	p-value
Ground glass	482 (87.3)	205 (87.2)	277 (87.4)	1	239 (88.2)	243 (86.5)	0.609
Acinar shadows	261 (47.3)	118 (50.2)	143 (45.1)	0.262	127 (46.9)	134 (47.7)	0.865
Bilateral / multilobar involvement							
Minimal	127 (23)	65 (27.7)	62 (19.6)	0.186	76 (28)	51 (18.1)	0.053
Mild	152 (27.5)	56 (23.8)	96 (30.3)		75 (27.7)	77 (27.4)	
Moderate	184 (33.3)	78 (33.2)	106 (33.4)		83 (30.6)	101 (35.9)	
Severe	44 (8)	17 (7.2)	27 (8.5)		17 (6.3)	27 (9.6)	
Single lobe	100 (18.1)	45 (19.1)	55 (17.4)	0.655	63 (23.2)	37 (13.2)	0.003
Peripheral distribution	455 (82.4)	192 (81.7)	263 (83)	0.735	233 (86)	222 (79)	0.034
Central distribution	280 (50.7)	111 (47.2)	169 (53.3)	0.169	131 (48.3)	149 (53)	0.307
Posterior distribution	450 (81.5)	194 (82.6)	256 (80.8)	0.658	222 (81.9)	228 (81.1)	0.827
Anterior distribution	325 (58.9)	136 (59.6)	189 (58.9)	0.727	153 (56.5)	172 (61.2)	0.262
Round opacities	89 (16.1)	43 (18.3)	46 (14.5)	0.243	54 (19.9)	35 (12.5)	0.02
linear opacities	41 (7.4)	17 (7.2)	24 (7.6)	1	14 (5.2)	27 (9.6)	0.052
Crazy paving	8 (1.4)	2 (0.9)	6 (1.9)	0.477	2 (0.7)	6 (2.1)	0.286
Reversed halo	9 (1.6)	4 (1.7)	5 (1.6)	1	6 (2.2)	3 (1.1)	0.332

Table 2. Inconsistent findings in HR CT-scan of symptomatic patients infected with coronavirus 2019

Findings	Total n=552 Frequency (%)	Female n=235 Frequency (%)	Male n=317 Frequency (%)	p-value	Age ≤50 n=271 Frequency (%)	Age >50 n=281 Frequency (%)	p-value
Tree-in-bud capacities	7 (1.3)	2 (0.9)	5 (1.6)	0.704	2 (0.7)	5 (1.8)	0.451
Centrilobular distribution	5 (0.9)	2 (0.9)	3 (0.9)	1	1 (0.4)	4 (1.4)	0.373
Peribronchovascular distribution	42 (7.6)	22 (9.4)	20 (6.3)	0.196	19 (7)	23 (8.2)	0.633
Predominantly nodular opacities	12 (2.2)	7 (3)	5 (1.6)	0.377	5 (1.8)	7 (2.5)	0.772
Cavitation	6 (1.1)	2 (0.9)	4 (1.3)	1	1 (0.4)	5 (1.8)	0.217
Lymphadenopathy	28 (5.1)	15 (6.4)	13 (4.1)	0.244	11 (4.1)	17 (6)	0.335
Pleural effusion	42 (7.6)	21 (8.9)	21 (6.6)	0.333	14 (5.2)	28 (10)	0.037

Figure 2. **A:** Bilateral and anterior to posterior peripheral ground glass opacities (white arrows). **B:** Ground glass opacity in upper lobe (black arrow) and consolidation in lower lobe of right lung (red arrow). **C:** Bilateral and peripheral ground glass opacities (white arrows). **D:** Consolidation in right lower lobe (black arrow). **E:** Right sided pleural effusion (red arrow). **F:** Bilateral and anterior to posterior peripheral ground glass opacities (white arrows) with peribronchovascular distribution in right middle lobe (black arrow). **G:** Bilateral and anterior to posterior peripheral ground glass opacities (black arrows). **H:** Small lymphadenopathies in middle mediastinum (white arrow).

Discussion

CT images with yielded 98% sensitivity play an important role in the diagnosis and evaluation of

COVID-19 and can be used as a standard method for rapid diagnosis of COVID-19 to manage patients [4-16]. The present study was conducted on 552 patients with clinical suspicion who referred for HRCT and had signs of involvement in the CT images. The most common suggestive findings in patients were ground glass opacity, peripheral distribution, and posterior distribution. The prevalence of ground glass opacity in the study population was 87.3%, which varied from 41% to 100% in other studies [9, 14, 17-28] and the prevalence of this finding was 67% given the difference in sample size in different studies and conducting the meta-analysis on these studies (Table 3). Peripheral distribution was the second most common finding in 82.4% of the study population. The prevalence of this finding in other studies ranged from 33% to 98% [15-21, 23, 25, 27, 28]. The meta-analysis conducted on the present study and other studies presented the peripheral distribution with 79% prevalence as the most common CT finding in these patients (Table 3).

The most common inconsistent findings in patients were pleural effusion, peribronchovascular distribution, and lymphadenopathy. Pleural effusion was 7.6% in the present study, which ranged between 2% to 9.7% in other studies, and the combination of the results of the present study and other studies estimated a 7% pleural effusion (Table 3). Lymphadenopathy in the CT scan was 5.1% higher than the value reported by other studies, such that this finding was not observed in two studies [15, 27] while it was 2.7% in one study [17] and 6% in another study. The total estimation was 4% (Table 3)

A halo sign of 1.6% was an uncommon finding in the present study, while other studies reported 11.1% to 64% [15, 20, 29]. The cumulative rate of the present study and other studies estimated a 41% rate of halo sign (Table 3). In addition, a similar situation occurred with crazy-paving as an uncommon finding in the present study which varied from 1.4% in this study to 12-89% in other studies [18-20 and 24]. The meta-analysis of the present study and other studies provided a rate of 32% for this finding.

Most CT findings in the present study showed no significant difference between genders and age groups, except for peripheral distribution, round opacities, single lobe, and pleural effusion, which showed a significant difference between the age groups under and over 50 years old. In a study by

Song et al., ground glass opacity and consolidative opacities were significantly different between age groups under and over 50 years old [28].

Mean age of participants was 51.2 ± 14.8 years. The male/female sex ratio was 1.38 Similar to the results of the present study, in a study conducted on 1,099 patients in China, the mean age of patients was 47 years, and the same sex ratio was observed [9].

The present study utilized an acceptable sample size which is one of the strengths of the present study. One of the weaknesses of the study is the lack of diagnostic confirmation by RT-PCR test, which was not possible for all patients due to the epidemic that occurred and the limited number of tests in Iran at the beginning of the epidemic. Other limitations of the study include the lack of a standard reporting format for the chest CT scans in these patients.

Table 3. CT-Scan findings in different study and pooled estimation of these findings

Author	Sample size	Ground-glass opacity	Peripheral distribution	Pleural effusion	Lymphadenopathy	Halo sign
Guan, WJ [9]	975	56.4				
Wu, J [14]	80	91.0				
Li, Y [15]	51		90.2	2.0	0.0	21.5
Bai, HX [17]	424	91.0	80.0	4.1	2.7	
Chung, M [18]	21	87.0	33.0			
Guan, CS [19]	47	100.0	93.6			
Han, R [20]	108	60.0	90.0			64.0
Liu, H [21]	59	72.0	98.0			
Liu, KC [22]	73	59.0		3.4		
Shi, H [23]	81	65.0	54.0			
Xu, X [24]	90	72.0				
Zhao, W [25]	101	86.1	87.1			
Zhu, W [26]	32	47.0				
Li, K [27]	56	80.4	87.5	8.9	0.0	
Song, F [28]	51	77		8	6	
Zhou, S [29]	62		77.4	9.7		
Yoon, SH [30]	9					11.1
Majidi, H (Present)	552	87.3	82.4	7.6	5.1	1.6
Pooled estimation (CI95%) with meta-analysis		67 (58-76)	79 (66-92)	7 (-24-39)	4 (-26-35)	41 (11-72)

Conclusion

Compared to other studies, the findings of the present study reported the peripheral distribution and ground glass opacity as important findings in the study population and by summarizing the results of studies, it can be concluded that peripheral distribution is the most common finding in these patients.

Declarations

Authors' Contributions

Hadi Majidi: Study design, Data collection, Writing of the paper, Final approval.

Elham-Sadat Bani-Mostafavi: Data collection, Writing of the paper, Final approval.

Zahra Mardanshahi: Data collection, Writing of the paper, Final approval.

Fanaz Godazandeh: Data collection, Writing of the paper, Final approval.

Roya Gasemian: Data collection, Writing of the paper, Final approval.

Keyvan Heydari; Data collection, Writing of the paper, Final approval.

Reza Alizadeh-Navaei: Study design, Data analysis, Writing of the paper, Final approval.

Ethics declarations

The study protocol was approved by the Ethics Committee of Mazandaran University of Medical Sciences (IR.MAZUMS.REC.1398.1425)

Patient Consent

Data was collected from PACS system and patient consent not applicable.

Conflict of interest

The authors declare that they have no conflict of interest.

Funding

This study was supported by Mazandaran University of Medical Sciences (Grant no: 7267).

References

1. Li H, Zhou Y, Zhang M, Wang H, Zhao Q, Liu J. Updated approaches against SARS-CoV-2. *Antimicrob Agents Chemother*. 2020. pii: AAC.00483-20. doi:10.1128/AAC.00483-20.
2. Chung M, Bernheim A, Mei X, Zhang N, Huang M, Zeng X, et al. CT Imaging Features of 2019 Novel Coronavirus (2019-nCoV). *Radiology*. 2020; 295(1):202-207. doi:10.1148/radiol.2020200230.
3. Lu R, Zhao X, Li J, Niu P, Yang B, Wu H, et al. Genomic characterisation and epidemiology of 2019 novel coronavirus: implications for virus origins and receptor binding. *The Lancet*. 2020; 395(10224): 565-574. doi: 10.1016/S0140-6736(20)30251-8.

4. Zhu N, Zhang D, Wang W, Li X, Yang B, Song J, et al. A novel coronavirus from patients with pneumonia in China, 2019. *N Engl J Med*. 2020; 382(8):727-733. doi:10.1056/NEJMoa2001017.
5. Su S, Wong G, Shi W, Liu J, Lai AC, Zhou J, et al. Epidemiology, genetic recombination, and pathogenesis of coronaviruses. *Trends Microbiol*. 2016; 24(6): 490-502. doi: 10.1016/j.tim.2016.03.003.
6. Cui J, Li F, Shi Z-L. Origin and evolution of pathogenic coronaviruses. *Origin and evolution of pathogenic coronaviruses. Nat Rev Microbiol*. 2019; 17(3):181-192. doi: 10.1038/s41579-018-0118-9.
7. Chan JF-W, Yuan S, Kok K-H, To KK-W, Chu H, Yang J, et al. A familial cluster of pneumonia associated with the 2019 novel coronavirus indicating person-to-person transmission: a study of a family cluster. *Lancet*. 2020; 395(10223):514-523. doi:10.1016/S0140-6736(20)30154-9.
8. Rodriguez-Morales AJ, Cardona-Ospina JA, Gutiérrez-Ocampo E, Villamizar-Peña R, Holguin-Rivera Y, Escalera-Antezana JP, et al. Clinical, laboratory and imaging features of COVID-19: A systematic review and meta-analysis. *Travel Med Infect Dis*. 2020: 101623. doi: 10.1016/j.tmaid.2020.101623.
9. Guan W-j, Ni Z-y, Hu Y, Liang W-h, Ou C-q, He J-x, et al. Clinical Characteristics of Coronavirus Disease 2019 in China. *N Engl J Med*. 2020. doi: 10.1056/NEJMoa2002032.
10. Wu J, Liu J, Zhao X, Liu C, Wang W, Wang D, et al. Clinical Characteristics of Imported Cases of COVID-19 in Jiangsu Province: A Multicenter Descriptive Study. *Clin Infect Dis*. 2020. pii:ciaa199. doi: 10.1093/cid/ciaa199.
11. Xie C, Jiang L, Huang G, Pu H, Gong B, Lin H, et al. Comparison of different samples for 2019 novel coronavirus detection by nucleic acid amplification tests. *Int J Infect*

- Dis. 2020; 93:264-267. doi: 10.1016/j.ijid.2020.02.050.
12. Ai T, Yang Z, Hou H, Zhan C, Chen C, Lv W, et al. Correlation of Chest CT and RT-PCR Testing in Coronavirus Disease 2019 (COVID-19) in China: A Report of 1014 Cases. *Radiology*. 2020: 200642. doi:10.1148/radiol.2020200642.
 13. Sun D, Li H, Lu XX, Xiao H, Ren J, Zhang FR, et al. Clinical features of severe pediatric patients with coronavirus disease 2019 in Wuhan: a single center's observational study. *World J Pediatr*. 2020. doi:10.1007/s12519-020-00354-4.
 14. Wu J, Wu X, Zeng W, Guo D, Fang Z, Chen L, et al. Chest CT Findings in Patients with Corona Virus Disease 2019 and its Relationship with Clinical Features. *Investigative radiology*. 2020. doi:10.1097/rli.0000000000000670
 15. Li Y, Xia L. Coronavirus Disease 2019 (COVID-19): Role of Chest CT in Diagnosis and Management. *AJR Am J Roentgenol*. 2020. doi:10.2214/AJR.20.22954.
 16. Ye Z, Zhang Y, Wang Y, Huang Z, Song B. Chest CT manifestations of new coronavirus disease 2019 (COVID-19): a pictorial review. *Eur Radiol*. 2020. doi: 10.1007/s00330-020-06801-0.
 17. Bai HX, Hsieh B, Xiong Z, Halsey K, Choi JW, Tran TML, et al. Performance of radiologists in differentiating COVID-19 from viral pneumonia on chest CT. *Radiology*. 2020: 200823. doi:10.1148/radiol.2020200823.
 18. Chung M. CT Imaging Features of 2019 Novel Coronavirus (2019-nCoV). *Radiology*. 2020; 295(1):202-7 10.1148/radiol.2020200463
 19. Guan CS, Lv ZB, Yan S, Du YN, Chen H, Wei LG, et al. Imaging Features of Coronavirus disease 2019 (COVID-19): Evaluation on Thin-Section CT. *Acad Radiol*. 2020. pii: S1076-6332(20)30143-4. doi:10.1016/j.acra.2020.03.002.
 20. Han R, Huang L, Jiang H, Dong J, Peng H, Zhang D. Early Clinical and CT Manifestations of Coronavirus Disease 2019 (COVID-19) Pneumonia. *AJR Am J*

- Roentgenol. 2020: 1-6. doi: 10.2214/AJR.20.22961.
21. Liu H, Liu F, Li J, Zhang T, Wang D, Lan W. Clinical and CT imaging features of the COVID-19 pneumonia: Focus on pregnant women and children. *J Infect.* 2020. pii: S0163-4453(20)30118-3. doi: 10.1016/j.jinf.2020.03.007.
 22. Liu KC, Xu P, Lv WF, Qiu XH, Yao JL, Gu JF, et al. CT manifestations of coronavirus disease-2019: A retrospective analysis of 73 cases by disease severity. *Eur J Radiol.* 2020; 126:108941. doi: 10.1016/j.ejrad.2020.108941.
 23. Shi H, Han X, Jiang N, Cao Y, Alwalid O, Gu J, et al. Radiological findings from 81 patients with COVID-19 pneumonia in Wuhan, China: a descriptive study. *Lancet Infect Dis.* 2020 ; 20(4):425-434. doi: 10.1016/S1473-3099(20)30086-4.
 24. Xu X, Yu C, Qu J, Zhang L, Jiang S, Huang D, et al. Imaging and clinical features of patients with 2019 novel coronavirus SARS-CoV-2. *Eur J Nucl Med Mol Imaging.* 2020; 47(5):1275-1280. doi: 10.1007/s00259-020-04735-9.
 25. Zhao W, Zhong Z, Xie X, Yu Q, Liu J. Relation Between Chest CT Findings and Clinical Conditions of Coronavirus Disease (COVID-19) Pneumonia: A Multicenter Study. *AJR Am J Roentgenol.* 2020: 1-6. doi: 10.2214/AJR.20.22976.
 26. Zhu W, Xie K, Lu H, Xu L, Zhou S, Fang S. Initial clinical features of suspected coronavirus disease 2019 in two emergency departments outside of Hubei, China. *J Med Virol.* 2020. doi: 10.1002/jmv.25763.
 27. Li K, Fang Y, Li W, Pan C, Qin P, Zhong Y, et al. CT image visual quantitative evaluation and clinical classification of coronavirus disease (COVID-19). *Eur Radiol.* 2020. doi: 10.1007/s00330-020-06817-6.
 28. Song F, Shi N, Shan F, Zhang Z, Shen J, Lu H, et al. Emerging 2019 Novel Coronavirus (2019-nCoV) Pneumonia. *Radiology.* 2020; 295(1):210-217. doi:10.1148/radiol.2020200274.

29. Zhou S, Wang Y, Zhu T, Xia L. CT Features of Coronavirus Disease 2019 (COVID-19) Pneumonia in 62 Patients in Wuhan, China. *AJR Am J Roentgenol.* 2020: 1-8. doi:10.2214/AJR.20.22975.
30. Yoon SH, Lee KH, Kim JY, Lee YK, Ko H, Kim KH, et al. (2020). "Chest Radiographic and CT Findings of the 2019 Novel Coronavirus Disease (COVID-19): Analysis of Nine Patients Treated in Korea." *Korean J Radiol.* 2020; 21(4):494-500. doi: 10.3348/kjr.2020.0132.

Figures

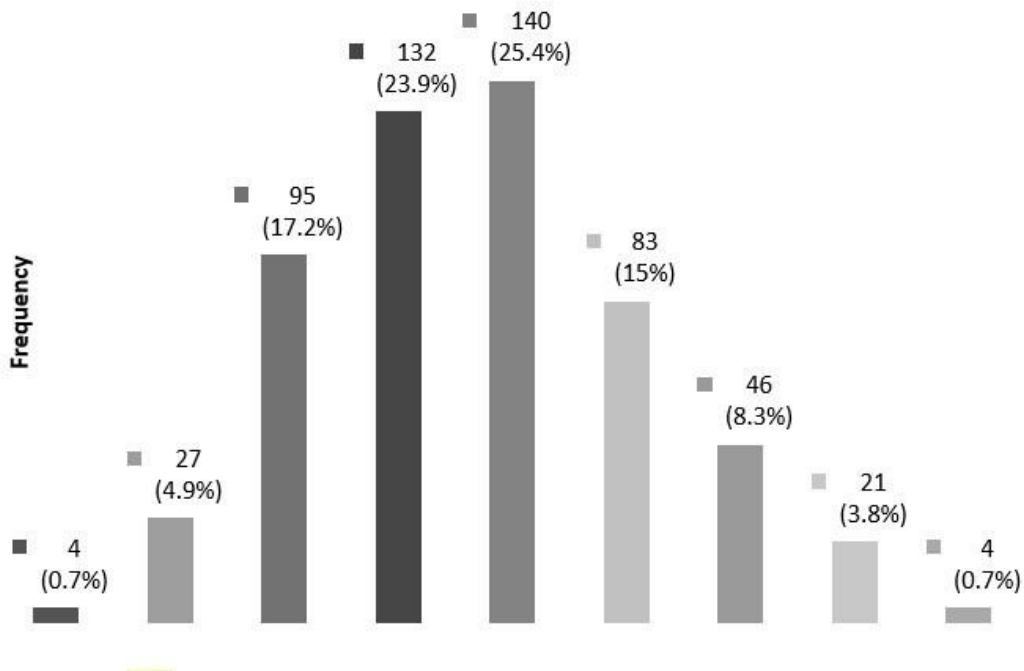


Figure 1

Age distribution of patients with coronavirus 2019

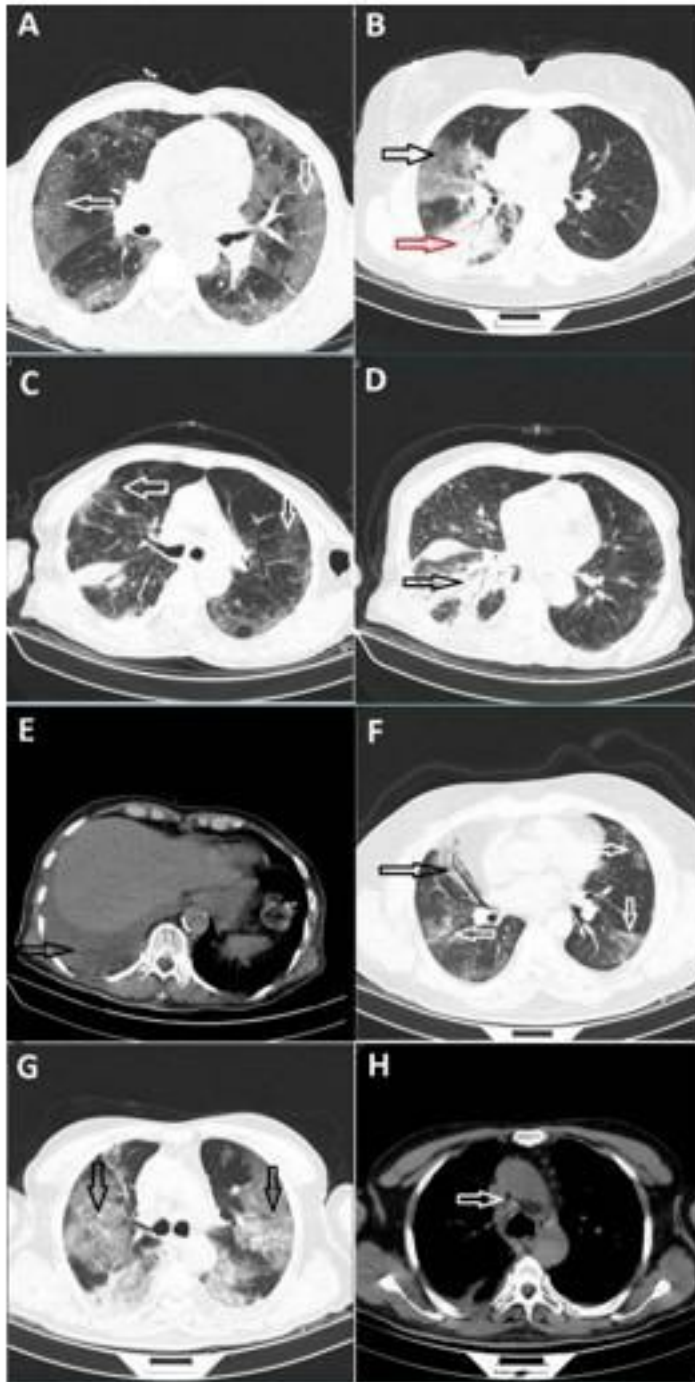


Figure 2

A: Bilateral and anterior to posterior peripheral ground glass opacities (white arrows). B: Ground glass opacity in upper lobe (black arrow) and consolidation in lower lobe of right lung (red arrow). C: Bilateral and peripheral ground glass opacities (white arrows). D: Consolidation in right lower lobe (black arrow). E: Right sided pleural effusion (red arrow). F: Consolidation in right lower lobe (black arrow) and ground glass opacities (white arrows). G: Bilateral peripheral ground glass opacities (white arrows). H: Consolidation in right lower lobe (white arrow).

Bilateral and anterior to posterior peripheral ground glass opacities (white arrows) with peribronchovascular distribution in right middle lobe (black arrow). G: Bilateral and anterior to posterior peripheral ground glass opacities (black arrows). H: Small lymphadenopathies in middle mediastinum (white arrow).